

# REDIM reduced modeling of quenching at a cold inert wall with detailed transport and different mechanisms

Christina Strassacker, Viatcheslav Bykov , Ulrich Maas  
Karlsruhe Institute of Technology, Institute of Technical Thermodynamics  
76131 Karlsruhe, Germany

## 1 Introduction

Simulations of reacting flow systems have become a powerful tool to study combustion processes. Quantitative predictions of combustion processes by using numerical methods leads to an improved understanding of combustion for optimization and control in various application aspects [1]. The combustion close to the wall is strongly influenced by the interaction between flame and wall and the arising trend towards downsizing (e. g. in internal combustion engines) increases the surface-to-volume ratio. Therefore, the influence of the wall rises and today's research focuses more on flame-wall-interactions.

In order to obtain reliable results very detailed models of chemical kinetics and of molecular diffusion are needed. In this respect, treating the detailed models of combustion in transient regimes requires robust model reduction to decrease CPU times and storage effort. The REDIM method [2] represents one of such methodologies (see e.g. [3, 4]). It performs model reduction both for detailed chemical kinetics as well as diffusion models. In this paper, the problem of a head-on flame quenching at cold wall [5] is studied both by using different detailed chemical reaction mechanisms [6–9] and transport models. The considered flame configuration allows to access the very complex problem in a simple geometry, to show how the REDIM approach works for transient regimes, compare and validate the results of different detailed models and of REDIMs.

## 2 Model configuration for flame-wall-interaction

The model system under consideration is comparable to corresponding experiments of Mann et al. [5] where a premixed laminar methane/air flame moves towards a cold wall and quenches due to heat losses. The system can be described by only one spatial coordinate. As a result, the one-dimensional reacting flow solver INSFLA [10] can be used to study the problem numerically.

The configuration and initial condition ( $t_1$ ) and evolution of the temperature for different time steps  $t_i$  ( $t_i < t_{i+1}$ ) are illustrated in Fig.1 (a). The unburnt gas in the left part of the domain is a stoichiometric

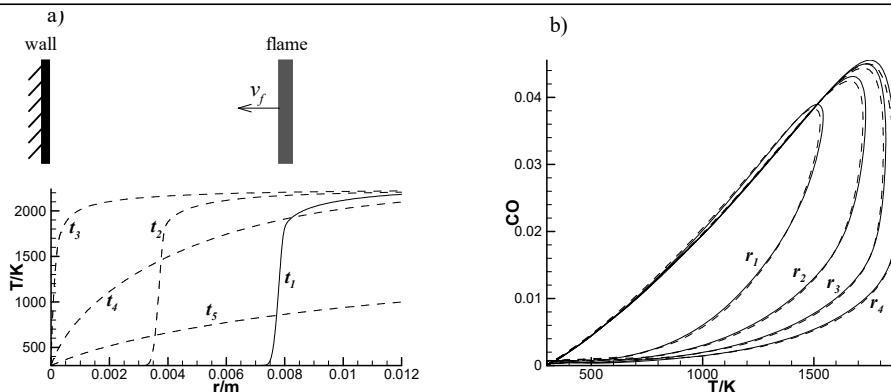


Figure 1: Left: configuration, initial condition ( $t_1$ ) and evolution of the temperature for different time steps  $t_i$  ( $t_i < t_{i+1}$ ); right: values of CO mass fraction over temperature  $T$  that occur at different positions  $r_i$  for the GRI mechanism. Detailed kinetics (solid line), reduced kinetics (dashed line). The positions are:  $r_1 = 0.2, r_2 = 0.3, r_3 = 0.4$  and  $r_4 = 0.5$  mm.

methane/air mixture at  $T = 300\text{K}$  and in the right part of the domain there are hot burnt gases. The pressure is considered to be constant at  $p = 1\text{bar}$  and the wall temperature is assumed to be constant at  $T_W = 300\text{K}$ . Furthermore, due to the low temperature the radical concentrations in the region close to the wall is very low, thus, heterogeneous reactions can be neglected [11]. In contrast to the previous work [12] which is based on a simplified transport model several detailed kinetic models and detailed transport mechanism with thermal diffusion are accounted for based on the Curtiss-Hirschfelder approximation [13]. This transport model is more detailed than transport modeling with unity Lewis-number or different Lewis-numbers and therefore, the presented approach can handle fuels with different constant Lewis-numbers as well. Under these assumptions, the boundary conditions at the wall are constituted by constant temperature  $T(r_W) = T_W$  and zero fluxes  $\frac{\partial j_i}{\partial x}(r_W) = 0$ , where the position of the wall is  $r_W = 0$  m and  $j_i$  is the diffusion flux of a species  $i$ . The right boundary conditions of the system are assumed to be zero gradients for all variables. The detailed chemical kinetics is described by four different mechanisms: GRI [6], Warnatz [7], Smooke [8] and San-Diego [9] mechanisms.

In order to compare the experimental results of Mann et al. [5] and the numerical results the mass fraction of CO over temperature  $T$  is investigated for different positions near the wall (such an illustration is shown in Fig.1 (b) for the GRI mechanism, see below for a detailed discussion).

### 3 Construction of the REDIM for flame-wall-interactions

The evolution equation of a reacting system is given by a system of partial differential equations for the state vector  $\Psi = (h, p, \frac{w_1}{M_1}, \dots, \frac{w_n}{M_n})^T$ , where  $h$  represents the specific enthalpy,  $p$  the pressure and  $\frac{w_i}{M_i}$  the specific mole fraction consisting of mass fraction  $w_i$  and the molar mass  $M_i$  of the species  $i$ . According to the method of the REDIM reduction the system state vector is reformulated as  $\Psi = \Psi(\theta)$ , with the parametrization vector  $\theta = (\theta_1, \theta_2, \dots, \theta_m)$ , where  $m \ll n + 2$ . The REDIM method is based on the assumption that only the time scales of a few reactive and diffusive processes overlap and need to be accounted for. The REDIM equation defines the manifold  $\Psi = \Psi(\theta)$ , while fast and slow processes are decoupled [2, 14]. It consequently accounts for both molecular transport and chemical reactions.

Table 1: different mechanisms used for REDIM-integration

Label	Number of species	Number of reactions	Ref.
GRI	53	325	[6]
Warnatz	34	165	[7]
Smooke	16	46	[8]
San-Diego	50	247	[9]

The usage of the detailed transport model complicates the REDIM evolution equation because the gradient estimate has to be accounted for in higher spatial derivatives, see e.g. [15] where it was shown how the problem can be overcome within the REDIM concept.

The combustion close to the wall is governed by at least two different processes: chemical reaction and heat loss. Therefore at least two progress variables have to be defined to characterize the extinction at the wall. The progress variable for the heat loss is chosen to be the enthalpy. For the progress of chemical reaction, a linear combination of specific mole numbers is considered for the different mechanisms of detailed chemical kinetics. The latter are shown with number of species and reactions for each mechanism in Tab. 1.

Before solving the REDIM evolution equation an initial guess for the manifold and a spatial gradient  $\text{grad}\Psi$  have to be defined. Both are obtained via detailed computations of the transient system, which were performed with INSFLA. Figure 2 (a) illustrates the mesh of the initial guess of the GRI mechanism. In order to integrate the REDIM evolution equation, Dirichlet boundary conditions are specified at the boundary of the REDIM. Therefore, the boundaries of the initial guess have to be constructed such that they account for the heat losses at the wall [12]. This is obtained by constructing the boundary of the REDIM with transient profiles from a detailed computation. Note, however, that Dirichlet boundary conditions are only used for simplicity and the use of more sophisticated boundary conditions are possible as well [16]. The REDIM evolution equation is integrated to a stationary state [2] for the different mechanisms and the necessary data for subsequent simulations are stored in REDIM-tables. Figure 2 (b) shows the REDIMs for the Smooke and the San-Diego mechanisms. The shapes of the REDIMs differ in the projections for  $\text{H}_2\text{O}_2$  (i. e. for minor species), whereas the REDIMs match quantitatively in most projections for major species.

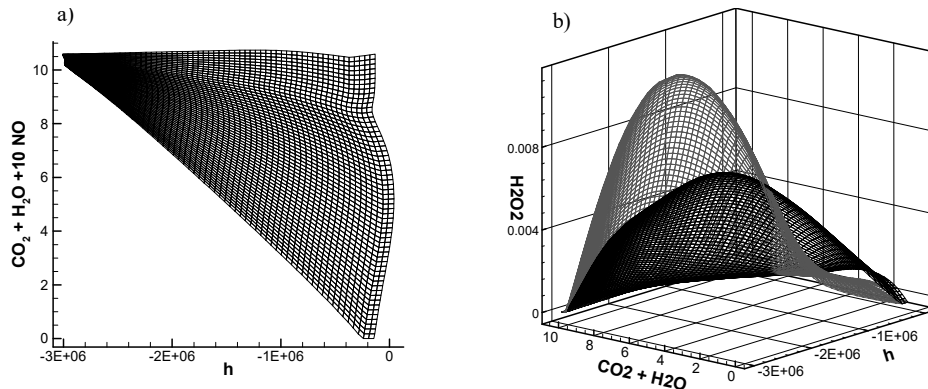


Figure 2: Left: mesh of the initial guess of the REDIM for the GRI mechanism projected onto enthalpy  $h$  (in  $\text{J kg}^{-1}$ ) and the sum of specific mole numbers of  $\text{CO}_2 + \text{H}_2\text{O} + 10 \cdot \text{NO}$  (in  $\text{kg mol}^{-1}$ ); right: mesh of the integrated REDIMs of the Smooke mechanism (grey mesh) and the San-Diego mechanism (black mesh) in state space onto enthalpy  $h$ , the sum of specific mole numbers of  $\text{CO}_2 + \text{H}_2\text{O}$  and  $\text{H}_2\text{O}_2$

## 4 Validation of the reduced model

The generated REDIM-tables for the different mechanisms are used in computations with the same model configuration. By the use of the REDIM-tables only two conservation equations have to be computed. The reduced conservation equations

$$\frac{\partial \theta}{\partial t} = \mathbf{S}(\theta) - \mathbf{U} \cdot \text{grad} \theta + \frac{1}{\rho} \Psi_{\theta}^{+}(\theta) \text{div}(\Xi(\theta) \text{grad} \theta) \quad (1)$$

are implemented in INSFLA. The terms  $\mathbf{S}(\theta)$ ,  $\Psi_{\theta}^{+}(\theta)$  and  $\Xi(\theta)$  are stored in the REDIM-table [2].

The boundary conditions for the species and temperature at the wall are determined by  $\frac{\partial j_{wCO_2}}{\partial t}(\theta(r_W)) = 0$ ,  $T(\theta(r_W)) = T_W$  and on the right boundary, zero gradients are applied. Starting from the same initial solution as the computations with detailed kinetics, the computations with reduced kinetics are performed with INSFLA and results are compared to the detailed computations. For this purpose, the mass fraction of CO over temperature  $T$  is investigated for different positions near the wall (such an investigation for experimental results was also carried out in Mann et al. [5]). Carbon monoxide is a pollutant and also an indicator for the completeness of a combustion process. Therefore, it is an important species to monitor. When the flame front travels by at a certain position, first the values of CO and temperature both increase, whereupon CO is consumed again. Figure 1 (b) shows such an illustration for the detailed and reduced kinetics of the GRI mechanism at different distances from the wall. The shown positions are very close and the temperature does not increase to high values because the flame is quenched. As it may be noticed, the reduced computations are in a very good agreement with the detailed computations for this mechanism. The illustrations for the Warnatz mechanisms, the Smooke mechanism and the San-Diego mechanism look qualitatively and quantitatively very similar to the illustration of the GRI mechanism and all reduced computations reproduce very well the progress of the combustion and the mass fraction of CO over temperature  $T$  curves.

### 4.1 Influence of the transport model

Figure 3 (a) shows the mass fraction of CO over temperature  $T$  of computations with reduced and detailed kinetics for the detailed molecular transport as well as the results for unity Lewis-number. Both reduced models reproduce very well the corresponding detailed solutions. In the late phase of cooling there are some differences in the case of unity Lewis-number, which does not occur in the case of the detailed molecular transport. Moreover, the curves of the different molecular transport models differ quantitatively whereby the curves for the detailed transport are closer to the experimental results of Mann et al. [5] where higher maximum temperatures were measured.

### 4.2 Influence of the mechanism

Quenching occurs when the heat flux  $q_w$  to the wall  $q_w = |-\lambda \frac{\partial T}{\partial r}|$  reaches its maximum, which is illustrated in Fig. 3 (b) for the GRI mechanism and the San-Diego mechanism. Therefore, this value can be used to verify the models, Fig.3 (b) shows that the heat flux for the reduced kinetics coincide well with the heat flux of the detailed kinetics of the same mechanism meaning that the propagation speed of the flame is reproduced quite well. Regarding the curve shapes of the different mechanisms they vary quantitatively,

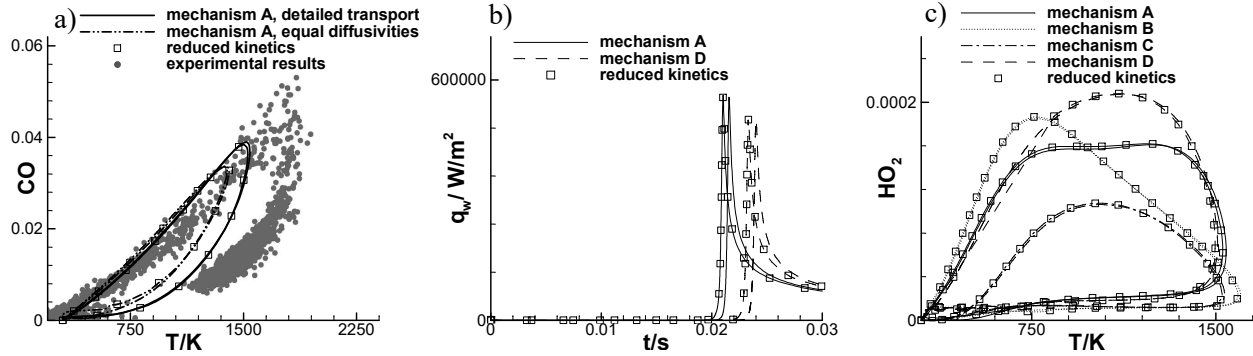


Figure 3: Left: values of CO mass fraction over temperature  $T$  that occur at the position  $r_i = 0.2$  mm for the GRI mechanism. The experimental results of Mann et al. [5] are illustrated as well; middle: Heat flux  $q_w$  to the wall; right: values of  $HO_2$  mass fraction over temperature  $T$  that occur at the position  $r_i = 0.2$  mm for the different mechanisms

which means that the propagation speed of the flame will differ for the different mechanisms. However, the values of mass fraction of CO over temperature  $T$  look quantitatively very similar for the different mechanisms and reduced and detailed kinetics. Even the mass fraction of the minor species  $HO_2$  is reproduced very well by the reduced kinetics compared for different detailed models (see Fig.3 (c)). Note, that there is a discrepancy of the computations of different mechanisms with the experimental results of Mann et al. [5], the measured temperature close to the wall in the experiments is higher than the computed temperature.

## 5 Summary and conclusions

In the current work the REDIM method for a system with heat loss was demonstrated for different mechanisms and for detailed molecular transport. The transient system behaviour of the considered model configuration can be reproduced very well. Even though the shapes of mass fraction of  $HO_2$  over  $T$  differ qualitatively for the different mechanisms (see Fig.3 (c)), there is a good agreement of corresponding reduced and detailed kinetics for the different mechanisms which means that the difference between different mechanisms is larger than the model reduction error. Furthermore, the computations with the detailed transport model agree better with the experimental results than the computations with unity Lewis-number. It was also illustrated that the detailed transport model shows a better consistency with the experimental results of Mann et al. [5].

## Acknowledgments

This research was supported by the Deutsche Forschungsgemeinschaft (DFG) within the SFB/Transregio 150.

## References

- [1] Warnatz J, Maas U, Dibble RW. (2001). Combustion (Vol. 3). Berlin: Springer.

- [2] Bykov V, Maas U. (2007). The extension of the ILDM concept to reaction-diffusion manifold. *Combust. Theory Model* 11 (6): 839-862.
- [3] Donini A, Bastiaans RJM, van Oijen JA, de Goey LPH. (2015). Differential diffusion effects inclusion with flamelet generated manifold for the modeling of stratified premixed cooled flames. *Proc. Combust. Inst.* 35(1): 831-837
- [4] van Oijen JA, Donini A, Bastiaans RJM, ten Thije Boonkkamp JHM, de Goey LPH. (2016). State-of-the-art in premixed combustion modeling using flamelet generated manifolds. *Progress in Energy and Combust. Science* 57: 30-74
- [5] Mann M, Jainski C, Euler M, Böhm B, Dreizler A. (2014). Transient flame-wall interactions: Experimental analysis using spectroscopic temperature and CO concentration measurements. *Combust. Flame* 161(9): 2371-2386.
- [6] Smith GP, Golden DM, Frenklach M, Moriarty NW, Eiteneer B, Goldenberg M, Bowman CT, Hanson RK, Song S, Gardiner Jr WC, Lissianski VV, Qin Z. (1999). GRI-Mech 3.0. <http://combustion.berkeley.edu/gri-mech/>
- [7] Stahl G, Warnatz J. (1991). Numerical investigation of time-dependent properties and extinction of strained methane and propane-air flamelets. *Combust. Flame* 85(3-4): 285-299.
- [8] Smooke MD, Puri IK, Seshadri K. (1988). A comparison between numerical calculations and experimental measurements of the structure of a counterflow diffusion flame burning diluted methane in diluted air. *Symp. (International) on Combust. (Vol. 21, No. 1: 1783-1792)*. Elsevier. [http://dx.doi.org/10.1016/S0082-0784\(88\)80412-0](http://dx.doi.org/10.1016/S0082-0784(88)80412-0).
- [9] Chemical-Kinetic Mechanisms for Combustion Applications, San Diego Mechanism web page, Mechanical and Aerospace Engineering (Combustion Research), University of California at San Diego, version 2011-11-22. <http://web.eng.ucsd.edu/mae/groups/combustion/mechanism.html>
- [10] Maas U, Warnatz J. (1988). Ignition processes in hydrogen-oxygen mixtures. *Combust. Flame* 74(1): 53-69.
- [11] Popp P, Baum M. (1997). Analysis of wall heat fluxes, reaction mechanisms, and unburnt hydrocarbons during the head-on quenching of a laminar methane flame. *Combust. Flame* 108(3): 327-348.
- [12] Steinhilber G, Bykov V, Maas U. (2016). REDIM reduced modeling of flame-wall-interactions: Quenching of a premixed methane/air flame at a cold inert wall. *Proc. Combust. Inst.* 36: accepted
- [13] de Charentenay J, Ern A. (2002). Multicomponent transport impact on turbulent premixed H<sub>2</sub>/O<sub>2</sub> flames. *Combust. Theory and Modelling*, 6(3): 439-462
- [14] Maas U, Pope SB. (1992). Simplifying chemical kinetics: Intrinsic low-dimensional manifolds in composition space. *Combust. Flame* 88(3): 239-264.
- [15] Maas U, Bykov V. (2011). The extension of the reaction/diffusion manifold concept to systems with detailed transport models. *Proc. Combust. Inst.* 33(1): 1253-1259
- [16] Neagos A, Bykov V, Maas U. (2016). Adaptive hierarchical construction of Reaction-Diffusion Manifolds for simplified chemical kinetics. *Proc. Combust. Inst.* 36: accepted